Advances in Science and Technology Research Journal

Advances in Science and Technology Research Journal 2023, 17(2), 53–62
https://doi.org/10.12913/22998624/161488
ISSN 2299–8624, License CC-BY 4.0

Received: 2023.02.01
Accepted: 2023.03.01
Published: 2023.04.01

Influence of the Curing Process on the Fatigue Strength and Residual Strength of a Fiber Composite Estimation Using the Theory of Markov Chains

Rafał Chatys[1], Mariusz Kłonica[2*]

[1] Faculty of Mechatronics and Machine Design, Kielce University of Technology, al. 1000-lecia P.P.7, 25-314, Kielce, Poland

[2] Faculty of Mechanical Engineering, Department of Production Engineering, Lublin University of Technology, ul. Nadbystrzycka 36, 20-618 Lublin, Poland

* Corresponding author's e-mail: m.klonica@pollub.pl

ABSTRACT

The paper deals with the influence of quality failure of matrix post-curing on the strength of such complex and difficult "new generation" materials as fiber composites, especially those with polymer matrix. The performed statistical analysis of the components determined the complexity of the layered composite structure. And the developed model of the weakest micro-volume presented in this paper has helped to describe not only the predictable strength of the laminate, but also the nature of failure, taking into account the fiber stresses and/or the distribution of end strains in the structure of the composite under consideration. The strength of fibre composite structures based on Markov chain theory takes into account technological aspects during the curing process. The presented model was verified on the basis of literature examples and experimental data obtained during the testing process. Numerical results show good agreement with literature examples and measured data. The presented model may represent a novel method that provides further insight into the curing process of epoxy resins.

Keywords: component of composite, destruction, fatigue strength, residual strength, curing process, Theory of Markov Chains.

INTRODUCTION

There is a very wide range of polymer matrix components on the market, which offer new opportunities in the design of fibre composite properties. At the same time, it forces us to develop new procedures for the moulding and manufacture of resin systems, especially the curing process [1, 2]. The improved strength properties of fibre composites are largely dependent on the polar structure of the epoxy ring (oxirane), which for epoxy resins is polyaddition [3] (or ionic polymerisation) based on the diglycidyl ether of bisphenol A (DGBEA) [4, 5]. Non-uniform curing of the resin system leads to degradation of the matrix or can result in incomplete curing due to non-compliance with reaction parameters (such as a non-linear increase in internal temperature due to the exothermic chemical reaction of the epoxy, leading to the so-called 'resin system life' being exceeded [6], or entrapment of volatiles or voids, respectively. The heat flow as a function of temperature [7, 8] (for DGEBA obtained from DSC scanning calorimetry) determines the nature of the curing reaction as a result of a multi-step reaction (due to the occurrence of gelation and glass transition [9, 10]).

It should be emphasised that the destruction process is most influenced by normal and tangential interlaminar stresses (τ), which visually cause the free edge to 'swell' [11, 12]. White and Hahn [13, 14] or Ciriscioli et al. [15] have proposed an optimal temperature cycle and algorithm that can reduce (minimise) the residual stresses and void inside the composite structure, respectively. In recent years, the understanding of the boundary effect [16, 17] as a result of these defects, has tended to focus on illustrating and bridging these phenomena [18], by replacing traditional open-mould composite fabrication methods [19, 20] (such as 'wet' lamination, spray-on resin system with chopped fibre, or long) with 'infusion under vacuum' moulding methods.

During the injection moulding process in vacuum methods, temperature and pressure affect the crystallisation kinetics of the polymer matrix, as a result of changes in the flow conditions in the plasticising system [21, 22]. Therefore, two rather important issues in modelling the flow of a resin system are often addressed in the literature:

- precise temperature history prediction [23–25], which prevents the resin system from turning into a gel before the mould is filled (or the resin system curing too quickly in the composite [26–28]);
- prediction and measurement of flow patency to determine with reasonable accuracy the temperature and velocity of the resin system in the mould [29–31].

Failure to meet technological parameters including the level of postcuring results in a higher probability of delamination at the edges of the specimens (especially in the layers [32]). Understanding this phenomenon in laminates leads to the analysis of ply alignment in the composite (and, thus, consideration of stress distributions in the structure [33]).

One option for describing damage accumulation through simple relationships using the static and fatigue properties of fibrous composites is Markov Networks [34]. However, such an application is not a new idea [35–37].

Random variables, or random vectors, describe static phenomena, whereas stochastic processes describe processes (phenomena) that change over time, as defined by the term 'chain' [38–40] (the discrete time parameter case, as opposed to the continuous parameter case, with which the term 'process' is associated). The fatigue process is discussed and addressed [41–45] in many stochastic (phenological) models.

Fractographic analysis using Macek [46, 47] method which employed roughness analysis is original attempt for fatigue fractures evaluations.

STRENGTH ASPECTS OF LAMINATE WITH CONSIDERATION OF THE MARKOV CHAIN THEORY

In the model, the fatigue failure of a specimen consisting of n fibres embedded in a matrix is based on the estimation of a certain critical micro-volume.

The elongated fibres, or fibre bundles (working in the elastic – rigid range) and the plastic matrix (in which plastic deformations accumulate during cyclic loading), work together. Markov chain theory [40] includes not only the work of the matrix, but the other layers of fibres working along the load (with different angles of alignment in the elastic range). Also in the model, it is assumed that with cyclic loading, the number r of elements working in the elastic range in the micro volume decreases by a certain value r_R (Table 1).

Table 1. Example of the structure of the transformation matrix of probabilities [27]

		j_Y	1			2			3		
		j_R	1	2	3	1	2	3	1	2	3
i_Y	i_R	i \ j	1	2	3	4	5	6	7	8	9
1	1	1	$p_{R0}p_{Y0}$	$p_{R1}p_{Y0}$	$p_{R2}p_{Y0}$	$p_{R0}p_{Y1}$	$p_{R1}p_{Y1}$	$p_{R2}p_{Y1}$	$p_{R0}p_{Y2}$	$p_{R1}p_{Y2}$	$p_{R2}p_{Y2}$
	2	2	0	$p_{R0}p_{Y0}$	$p_{R1}p_{Y0}$	0	$p_{R0}p_{Y1}$	$p_{R1}p_{Y1}$	0	$p_{R0}p_{Y2}$	$p_{R1}p_{Y2}$
	3	3	0	0	1	0	0	0	0	0	0
2	1	4	0	0	0	$p_{R0}p_{Y0}$	$p_{R1}p_{Y0}$	$p_{R2}p_{Y0}$	$p_{R0}p_{Y1}$	$p_{R1}p_{Y1}$	$p_{R2}p_{Y1}$
	2	5	0	0	0	0	$p_{R0}p_{Y0}$	$p_{R1}p_{Y0}$	0	$p_{R0}p_{Y1}$	$p_{R1}p_{Y1}$
	3	6	0	0	0	0	0	1	0	0	0
3	1	7	0	0	0	0	0	0	1	0	0
	2	8	0	0	0	0	0	0	0	1	0
	3	9	0	0	0	0	0	0	0	0	1

Understanding the destruction of a sample as a stationary Markov chain process in which the states are defined by the number of destroyed elements along the axis (case A) and the number of plasticity boundaries with some value r_Y (case B), the probability transformation matrix can be represented as a set with (r_Y+1) blocks with (r_R+1) internal states of each. The indices i and j of the input and output states, respectively, are expressed as parts of the local indices i_Y, i_R, j_Y, j_R. We assume binomial and log-normal distributions for the damaged elements operating in the elastic range and in the plastic range, respectively (one step at a time).

In contrast, the probability transition matrix (1), in which all probabilities below the diagonal are zero, describes the fatigue strength. Selected probabilities can form conditional probabilities.

$$P = \begin{bmatrix} q_1 & p_1 & 0 & & & \dots & 0 \\ 0 & q_2 & p_2 & 0 & & \dots & 0 \\ 0 & 0 & q_3 & p_3 & 0 & \dots & 0 \\ \dots & \dots & \dots & \dots & \dots & \dots & \dots \\ 0 & & & \dots & q_r & p_r & 0 \\ 0 & & & \dots & 0 & 0 & 1 \end{bmatrix} \tag{1}$$

where: $q_i = 1 - p_i$, $i = 1,\dots,r$:

In this Markov chain there are r irreversible states and one absorbing state. Whereby the r irreversible states are treated as r defects, the accumulation of which leads to the destruction of some critical micro-volume (the Markov chain reaches the absorbing state).

The generated probabilities of the variable T (i.e. the inverse of the transformation – Table 2) are defined by relation (6) and (7) with the cumulative distribution function (8), respectively. The model parameters are shown in Table 2.

Consider that the product of the matrix P^i (9) and the vector b gives the column vector of the fatigue strength distribution. fatigue strength, the elements of which correspond to the initial (starting) states of the Markov chain ($F^{(1)}$ (t). $F^{(2)}$ (t),....$F^{(r)}$ (t)). In the general case, it can be used to determine the fatigue strength distribution function with a given probability distribution in the starting states π (π if known, the fatigue strength distribution function has the form in the initial conditions p):

$$F_t(t) = \eta \, P^t \, b \, (\eta) \tag{10}$$

Table 2. Model parameters [45]

Characteristics	Dependencies
Fatigue strength (time to absorption)	$T = X_1 + X_2 + \dots + X_r$ (2) where: X_i, i = 1; r – time of destruction (is) in an i-m state.
Random variable X_i in a geometric distribution	$P(X_i = n) = (1 - p_i)^{n-1} p_i$ (3)
Expected value	$E(X_i) = 1/p_i$ (4)
Dispersion	$V(X_i) = (1 - p_i)/p_i^2$ (5)
Random variable	$E(T) = \sum_{i=1}^{r} 1/p_i \qquad V(T) = \sum_{i=1}^{r} (1 - p_i)/p_i^2$ (6)
A function that generates the probabilities of a random variable T	$G_T(z) = \sum_{i=0}^{\infty} p_T(i) \cdot z^i \prod_{i=1}^{\infty} \frac{z \; p_i}{1 - z(1 - p_i)}$ (7)
Cumulative distribution function	$F_T(t) = p_{1\ r+1}(t)$, t = 1, 2, 3 (8) where: $p_{1\ r+1}(t)$ is (1, r + 1) – matrix element
Fatigue strength distribution function	$P(t) = P^t$ (9) described as: $F_T(t) = aP^t b$ where: a = (100…0); b = (00…01)T – column vector

The problem for consideration is to find the relationship between the probabilities, $p_i = 1,...,r$ with the values of the static strength distribution of the composite elements and the fatigue loads, respectively. It is assumed that in the first step of the Markov chain (e.g. 1 or 1000 cycles) one element fails. If there are still working (R-i) parallel components (having one and the same distribution function), the static strength F(s), then the probability of the next failure (of the remaining components) is equal:

$$p_i = 1-(1-F(s_i))^{R-i} \tag{11}$$

where: R – initial number of elements;
i – number of destroyed elements;
s_i – stress (load on one element), corresponding to a uniform load distribution among the remaining (R-i) elements.

We assume that in the general case:

$$s_i = \frac{SR = iS_f}{R-i} = \frac{S(1-iS_f/RS)}{1-i/R} \tag{12}$$

where: S – the initial (in the first step of the process) load in each component;
S_f – the average stress that can still carry the load (at least at the beginning of the working components of the composite – the cumulative failure of the component that occurs in different sections).

If all the model parameters are known (formulas 5, 7, 9), we can calculate the fatigue curve. Under the assumption that one step in the Markov chain corresponds to kM cycles, we use a modified formula:

$$\begin{gathered} E(T) = k_M \sum_{i=1}^{r} 1/p_i, \\ V(T) = k_M^2 \sum_{i=1}^{r} (1-p_i)/p_i^2 \end{gathered} \tag{13}$$

In this study, a log-normal strength distribution was assumed:

$$F(s) = \Phi((g(s)-\theta_0)/\theta_1) \tag{14}$$

where: $\Phi(.)$ is a function of the standard normal distribution,
g(s)=log(s)

The model under consideration is now defined in the general case by the constant $\eta = (\theta_0, \theta_1, r, R, k_M, S_f)$, having in the general case 6 components, where: θ_0, θ_1 – parameters of the static strength distribution of the composite elements (expected value and standard deviation of the strength logarithm); R – number of elements in the "critical volume" of the composite, the failure of which means complete failure of the specimen; r – critical number of elements in the laminate (the value of r has a significant impact on the dispersion and fatigue strength variation factor); relationship $\rho = r/R$ approximates the amount of damage (proportion of damage) in the specimen cross-section corresponding to the total failure of the specimen; k_M – number of cycles corresponding to one step of the Markov chain; S_f – residual strength of already damaged (in other sections) elements (this value depends on the number of layers and their orientation, or the properties of the matrix).

LOCAL STRESSES WITH ESTIMATED FATIGUE CURVE EQUATION AND RESIDUAL STRENGTH

The local stress in the model was determined by the number of destroyed elements working in the elastic range (such as case A, or case B), and the fatigue curve is determined by renumbering the states the composite is in [45].

After the destruction and elements working in the elastic range, the new value of this cross-section (Table 3, relation 15) is $f_{Ri} = f_R(1\text{-}i/r_R)$, and the probability transformation matrix takes the form 16 with four conditions (Table 3).

EXPERIMENTAL DATA PROCESSING

In this study, the object of the research was a 4 – layer laminate moulded using the method of pressurised injection of a resin system (by sucking) into a mould using the vacuum bagging method (Vacuum bagging). The composition and technological parameters of the moulded 4 – layer composite are illustrated in Table 4.

The bisphenol A-based epoxy matrix is characterised by very low viscosity, excellent mechanical properties, chemical properties and thermal strength (Table 5).

Table 3. Estimation of fatigue curve and residual strength by the values of local stressesd

Parameters	Description
Local stresses	The cross-sectional area of the part (working in the plastic range) = const only its length depends on the number of elements that have reached the yield point. If both parts work in the elastic range, the equilibrium equation is of the form: $\begin{cases} S_R \cdot f_R + S_Y \cdot f_Y = S \cdot f, \\ \dfrac{S_R}{E_R} = \dfrac{S_Y}{E_Y}, \end{cases}$ (15) where: *S* – average normal stress, *E* – modulus of elasticity, where the subscripts R and Y stand for parts operating in the elastic and plastic ranges, respectively.
Fatigue curve equation	$P = \begin{array}{c} \begin{array}{cc} r-s & s \end{array} \\ \begin{bmatrix} I & O \\ R & Q \end{bmatrix} \end{array} \begin{array}{l} \}r-s \\ \}\ s \end{array}$ (16) where: *Q* – is a stochastic matrix describing the probability of transformation only among transients, *I* – is a matrix of unity, 0 – is a matrix containing the zeros (r-s) by s, R – is a matrix describing the probability of transformation from transition states to absorbing states in one step. It can be shown that the probability transformation matrix with *k* – degrees P^k takes the form: $\left\{p_{ij}^{(k)}\right\} = P^k = \begin{bmatrix} I & O \\ R' & Q^k \end{bmatrix}$, (17) Components (i, j) of the matrix Q^k describe the probability of reaching a transition state S_j after exactly k steps starting from the (transitional) state S_i.
Conditions of the model	
1. $N = \{E(T_{ij})\} = (I-Q)^{-1}$ 2. $\tau = \{E(T_{ij})\} = N\xi$, where: $\xi = [1,\ldots,1]'$ is a columnar vector of units, 3. $\tau_2 = (2N - I)\tau - \tau_{sq}$ where: $\tau_{sq} = \{(E(T_i))^2\}$. 4. $B = NR$. where: T_{ij} – is the number of visits to state j, starting from state *i,* T_i – is the absorption time (including the initial state) starting from state *i*, *E(Ti), Var(Ti)* – is the mean I variance of the absorption time if i is the state of the initial state, $\tau = \{E(T_{ij})$, $\tau_2 = \{Var(T_i)\}$ – are corresponding column vectors, and is the index of the transition state, $B = \{b_{ij}\}$ – is a matrix of absorption probabilities, b_{ij} – is the probability that the process will be absorbed in state j if the initial state is *i*.	
$\tau = N \cdot \xi$, (18) where: $N = (I-Q)^{-1}$ base matrix of probabilities of states initial states; determines the expectation value and variations of the absorption time, ξ – is a column vector filled with 1.	

From the fabricated 4-ply glass/epoxy laminate with an average thickness of 1.8 ÷ 2.0 mm, specimens (according to EN 10002–1+ACI with a 200 mm measuring base) were cut for static tensile testing on a SHIMADZU AGX-V 20kN machine at a speed of 2 mm/min.

In order to determine the effect of the postcuring process, the rest of the samples were tested, respectively, by subjecting them to UV lamps at 60°C (with light of 0.76W·m^{-2} × nm^{-1} at 340 nm wavelength) and additional annealing at 50°C for 4h in accordance with ISO 4892–3 and the manufacturer's recommendations.

RESULTS

The average strength of the 4-layer composite (from 5 samples – according to DIN-EN ISO 527) after accelerated postcuring with the UV QUV (Q-Lab QUV accelerated postcuring tester) improved by approx. 18% (*S* = 126.47 MPa; Table 6),

Table 4. Technological parameters and components of a laminate moulded by the vacuum bagging method

Components of 4-layer laminate		
1.	Reinforcement, %	150 g/m^2 glass fabric (PLAIN linen weave) with silicone preparation
2.	Matrix, %	epoxy resin LH 288, 50
3.	Hardeners	H 505
Technological parameters of the 4-layer laminate		
4.	Time of deformation, h	24
5.	Gelation time, h (°C)	1.5 (23)
6.	Aftercare, °C (h)	50 (10)

which cannot be said for the average strength of the samples before postcuring (S = 103.58 MPa). In addition, the tests revealed a smaller scatter in strength after accelerated postcuring on the tester (8%) than the samples before accelerated postcuring (10–11%).

Postconditioning with 24 h fluorescence light from UV lamps in parts of the UVA, UVB and UVC spectrum for a moulded polymer matrix composite material showed a beneficial effect on the strength properties, related to the plasticisation of the matrix. The source of this behaviour is their complex microstructure [48], which makes polymers at the molecular level (i.e. chains, network rings and their crystalline, amorphous and mixed combinations) sensitive to the effects of temperature, visible and ultraviolet light as well as water (moisture), atmospheric and chemical pollutants.

The deterioration process of the components of the composite structure as well as the composite itself should be complemented by an analysis of the influence not only of the load, but also of atmospheric (operational) factors that complete the sequential accumulation of damage. Having a well-cross-linked (post-cured) laminate, we can determine the influence [49–50] of aggressive factors (such as sulfur di- and trioxide SO_2 and SO_3, nitrogen oxides and carbon oxides), which in combination with moisture are inorganic acids. Also, during aging (which is a process of structural changes that occur in the polymer under the influence of long-term external factors) under natural climatic conditions, it is most often difficult to distinguish which factor has the dominant influence, as they act simultaneously. All the above-mentioned chemical transformations are very complex and often proceed simultaneously.

Table 5. Properties of LH 288 epoxy resin [36]

Condition	Fluid
Epoxy equivalent, g/mol	180–196
Colour (Gardner)	Max 3
Epoxy index, mol/1000g	0.51–0.56
Flash point, °C	over 150
Viscosity at 25°C, mPa·s	500–900
Density, g/cm^3	1.12–1.16

Estimation of residual strength

Assuming that one step in the Markov chain corresponds to k_M cycles (then k_M is also an element of the vector η) n the cyclic load, and the column vector of the average number of steps before the transformation (with different initial states – transitions), can be determined by equation 18 (see Table 3 [33]). The variance vector (equation 19) in the probability matrix (equation 20) in the absorbing state (i.e., the components of the first row of matrix B) show the probability of different types of destruction (of elements operating in the elastic range with unacceptable elongation of the specimen in the plastic range, or under conditions of a combination of these destructive factors).

$$\tau_2 = (2N - I)\tau - \tau_{sq} \qquad (19)$$

where: $\tau_{sq}(i) = (\tau(i))^2, i \in I_A$,
I_A – is a sequence of indices of irreversible states.

$$B = \{B_{ij}\} = NR \qquad (20)$$

where: B_{ij} – is the probability in the absorbing state of the process at the j-th state of the transformation, if the initial state is the i-th irreversible state.

Fatigue strength $t_p(S)$ determines the number of cycles through equation 21, (i.e., the probability p of destruction at the initial normal stress S – fatigue curve),

Table 6. Mechanical properties of the sandwich composite obtained by the vacuum bag method

No specimens	ε, mm	S_{max}, MPa	*E*, GPa
Before accelerated postcuring of the laminate			
A–11	1.56	108.01	5.92
A–12	1.64	105.85	6.14
A–13	1.74	95.94	5.54
A–14	1.79	92.72	5.24
A–15	1.48	115.37	6.12
Average	1.64	103.58	5.79
After accelerated postcuring of the laminate with fluorescent light in parts of the spectrum of the UVA, UVB i UVC			
A–21	1.70	117.47	6.56
A–22	1.84	121.96	6.65
A–23	1.87	126.17	6.76
A–24	2.05	136.80	6.92
A–25	1.93	129.94	6.83
Average	1.88	126.47	6.74

$$t_p(S) = k_M F_{T_A}^{-1}(p; S, \eta) \tag{21}$$

while the vector of probabilities after n1 steps with stress S1, is defined as (only on unstressed specimens):

$$\pi_{S_1 n_1} = (1, 0, \ldots) P_1^{n_1} \tag{22}$$

The components of the probability distribution vector of unabsorbed (irreversible) Markov chain states are:

$$\pi^*_{S_1 n_1}(k) = \pi_{S_1 n_1}(k) / \sum_{m=1}^{m^*} \pi_{S_1 n_1}(m) \tag{23}$$

where: $\pi_{S_1 n_1}(k)$, k=1,…,
m^* – components of the vector $\pi_{S_1 n_1}$;
$m^* = (r_Y+1)(r_R+1) - (r_Y+1+r_R)$ – is the total number of unabsorbed (irreversible) states.

The last (r_Y+1+r_R) components of the vector π_{n1}^*, corresponding to the transformation states are equal to zero, since only specimens that were not destroyed after preloading were considered. For

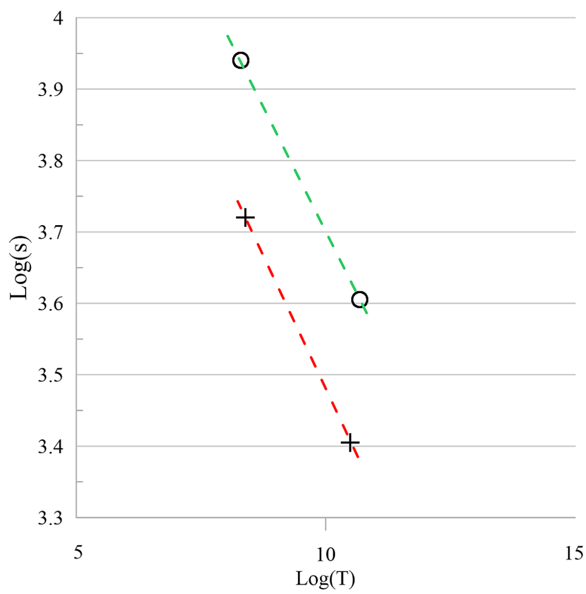

Fig. 1. Estimation of the average fatigue strength of laminate before (+) and after accelerated postconditioning (o) for two stresses (S_1, n_1) =31.07 (38.98) MPa for 30000 cycles; (S_2, n_2) = 41.43 (51.98) MPa for 10000 cycles, respectively

Tabel 7. Model parameters

Parameters	Values
Mean value of strength of the longitudinal elements, (L_R)*	4.6403 (4.8400)
$R = exp(L_R)$, MPa	103.58 (126.47)
Mean standard deviation (Std_{RP}) of strength of the longitudinal elements in logarithmic coordinates	0.1
Number of longitudinal elements in critical volume (r_{RP})	2
The relative value of the surface area of the working longitudinal elements in WMK (f_{RO})	0.65–0.70
Number of cycles equivalent to one step in a Markov chain (k_m)	1265

Note: * calculations in the natural logarithm.

Table 8. Modeled residual strength values of 4-ply laminate

Residual strength values of laminate at asymmetry R = 0.1			
No	The level of load (K), MPa	Before accelerated postconditioning, S_R,MPa	After accelerated postconditioning, S_R, MPa
1	at $K = 0.3$	116.21	123.32
2	at $K = 0.4$	125.37	151.76

such specimens, the stress distribution function σ_{n1}^{II}, at which there is a transition in one step of the Markov chain (corresponding to the destruction of the sample in the k_M cycles), takes the form of:

$$F_{\sigma_{n1}}(x) = \pi^{*}_{S_1 n_1} P(x) b \quad (24)$$

where: $x \geq S_1$, $P(x)$ – is the probability transformation matrix at $S = x$.

Estimating the fatigue average $E(T(S))$ at any S (Table 7) allows to reproduce the fatigue curve quite accurately, that is to match (Fig. 1) the fatigue curve data (T-N) with experimental results from the number of initial loads at two stress levels $K * S_{statist}$ ($K_{0.1} = 0.3; 0.4$).

It can be seen that with the selected parameters of the model for lower stresses (Table 7, where ((S_1, n_1) = 31.07 MPa, 30000), and at higher stress significances ((S_2, n_2) = 41.43 MPa, 10000) after accelerated postconditioning, we observe a slight increase in residual strength (Table 8) than before accelerated postconditioning (the effect depends on the duration of cyclic loading, i.e. the number of cycles).

For this purpose, it was assumed that the number of cyclic loads with fairly large values of is approximately equal to the minimum significance of fatigue strength at a certain load level obtained from calculations.

CONCLUSIONS

This paper presents a model for estimating the strength of a fibrous composite based on the critical micro-volume with consideration of the distribution of strength properties and degree of cure before and after accelerated post-curing with 24-hour fluorescent light from UV lamps in the UVA, UVB and UVC parts of the spectrum, of a laminate using the vacuum bag method. The model was validated against literature and experimental data.

The average strength composite after accelerated postcuring with the UV QUV improved by approx. 18%, compared to samples before postcuring. In addition, the tests revealed a smaller scatter in strength after accelerated postcuring amounting to 8% than the samples before accelerated postcuring (10–11)%.

The nonlinear internal heat source and heat transfer process result in inhomogeneity of temperature and degree of cure inside the epoxy part. This work therefore provides a preliminary yet novel method to provide further insight into the curing process of the epoxy resin, which can improve the mechanical and performance properties of the finished part by reducing deformation and residual stresses during the curing process.

REFERENCES

1. Markuszewski, D., Bielak, M., Wądołowski, M., Grzybek, A. Polymer-Carbon Composite Supporting Structure. Advances in Science and Technology Research Journal 2022; 16(6): 244–250. https://doi.org/10.12913/22998624/156300
2. Markuszewski, D., Wądołowski, M., Gorzym, M., Bielak, M. Concept of a Composite Frame of Martian Vehicle. Advances in Science and Technology

Research Journal 2021; 15(4): 222–230. https://doi.org/10.12913/22998624/141213

3. Lakho, D.A., Yao, D., Cho, K., Ishaq, M., Wang, Y. Study of the Curing Kinetics toward Development of Fast-Curing Epoxy Resins. Polym.-Plast. Technol. Eng. 2017; 56: 161–170.
4. Bereska, B., Iłowska, J., Czaja, K., Bereska, A. Hardeners for epoxy resins. Chemical industry 2014; (4)93: 443–448.
5. Zhang, J., Xu, Y.C., Huang, P. Effect of cure cycle on curing process and hardness for epoxy resin. Polymer 2009; 3(9): 534–541.
6. Kłonica, M., Kuczmaszewski, J., Samborski, S. Effect of a notch on impact resistance of the epidian 57/Z1 epoxy material after “Thermal Shock”. Solid State Phenomena 2016; 240: 161–167. https://doi.org/10.4028/www.scientific.net/SSP.240.161
7. Ren, R., Chen, P., Lu, S., Xiong, X., Liu, S. The curing kinetics and thermal properties of epoxy resins cured by aromatic diamine with hetero-cyclic side chain structure. Thermochim. Acta 2014; 595: 22–27.
8. Jianfeng, D., Shangbin, X., Dongna, L. Numerical Analysis of Curing Residual Stress and Deformation in Thermosetting Composite Laminates with Comparison between Different Constitutive Models. Materials 2019; 12(4): 572. https://doi.org/10.3390/ma12040572
9. O’Brien, D.J., Mather, P.T., White, S.R. Viscoelastic properties of an epoxy resin during cure. J. Compos. Mater. 2001; 35: 883–904.
10. Kłonica, M., Kuczmaszewski, J. Modification of Ti6Al4V titanium alloy surface layer in the ozone atmosphere. Materials 2019; 12(13). https://doi.org/10.3390/ma12132113
11. Gnatowski, A. Influence of the type of filler on the properties of selected polymer mixtures. Quarterty “Composites theory and practice” 2005; 2: 63–68.
12. Wang, X.X.; Zhao, Y.R.; Su, H.; Jia, Y.X. Curing process-induced internal stress and deformation of fiber reinforced resin matrix composites: Numerical comparison between elastic and viscoelastic models. Polym. Polym. Compos. 2016; 24: 155–160.
13. White, S.R., Hahn, H.T. Process modeling of composites materials: Residual stress development during cure. Part I. Model formulation. Journal of Composite Materials 1992; 26(16): 2402–2422.
14. White, S.R., Hahn, H.T. Process modeling of composites materials: Residual stress development during cure. Part II. Experimental validation. Journal of Composite Materials 1992; 26(16): 2423–2453.
15. Ciriscioli, P.R., Wang, Q., Springer, G.S. Autoclave curing – Comparisons of model and test results, Journal of Composite Materials 1992; 26(16): 90–102.
16. Chatys R. Modeling of Mechanical Properties with the Increasing Demands in The Range of Qualities and Repeatability of Polymers Composites Elements, Monograhy na Polymers and Constructional Composites, Gliwice 2008; 36–47.
17. Maria, B., Lionel, M., Alice, C., Martin, L., Edu, R. Numerical analysis of viscoelastic process-induced residual distortions during manufacturing and post-curing. Compos. Part A Appl. Sci. Manuf. 2018; 107: 205–216.
18. Maria, B., Lionel, M., Alice, C., Martin, L., Edu, R. Numerical analysis of viscoelastic process-induced residual distortions during manufacturing and post-curing. Compos. Part A Appl. Sci. Manuf. 2018; 107: 205–216.
19. Tavakol, B., Roozbehjavan, P., Ahmed, A., Das, R., Joven, R., Koushyar, H. Prediction of Residual Stresses and Distortion in Carbon Fiber-Epoxy Composite Parts Due to Curing Process Using Finite Element. J. Appl. Polym. Sci. 2013; 128: 941–950.
20. Fragassa, C., de Camargo, F.V., Pavlovic, A., Minak, G. Explicit numerical modeling assessment of basalt reinforced composites for low-velocity impact. Compos. Part B Eng. 2019; 163: 522–535.
21. Kozioł M. Pressure-vacuum saturation of stitched and three-dimensionally woven glass fiber preforms. 2016, Wyd. PŚ. Gliwice 2016.
22. Ma, Y.R., He, J.L., Li, D., Tan, Y., Xu, L. Numerical simulation of curing deformation of resin matrix composite curved structure. Acta Mater. Compos. Sin. 2015; 32: 874–880.
23. Deléglise, M., Binétruy, C., Castaing, P., Krawczak, P. Use of non local equilibrium theory to predict transient temperature during non-isothermal resin flow in a fibrous porous medium. Int. J. Heat Mass Transf. 2007; 50: 2317–2324. DOI: 10.1016/j.ijheatmasstransfer.2006.10.020
24. Hsiao, K., Laudorn, H., Advani, S.G. Experimental investigation of heat dispersion due to impregnation of viscous fluids in heated fibrous porous during composites processing. ASME J. of Heat Transfer 2001; 123: 178–187.
25. Chiu, H., Yu, B., Chen, S.C., Lee, L.J. Heat transfer during flow and resin reaction through fiber reinforcement. Chemical Engineering Science 2000; 55: 3365–3376.
26. Hsiao, K.T., Advani, S.G. Modified effective thermal conductivity due to heat dispersion in fibrous porous media, Int. J. Heat Mass Transfer 1999; 42: 1237–1254.
27. Henne, M., Ermanni, P., Deleglise, M., Krawczak, P. Heat transfer of fiber beds in resin transfer molding: an experimental approach. Composites Science and Technology Pergamon, Elsevier Sci. Ltd., UK 2014; 64.

28. Ganapathi, A.S., Joshi, S.C., Chen, Z. Simulation of Bleeder flow and curing of thick composites with pressure and temperature dependent properties. Simul. Model. Pract. Theory 2013; 32: 64–82.
29. Choi, M.A., Lee, M.H., Chang, J., Lee, S.J. Permeability modeling of fibrous media in composite processing. Journal of Non-Newtonian Fluid Mechanics 1998; 79: 585–598.
30. Starov, V.M., Zhdanov, V.G. Effective viscosity and permeability of porous media. Colloids and Surfaces 2001; 192: 363–375.
31. Kim, S.K., Opperer, J.G., Daniel, I.M. Determination of permeability of fibrous medium considering inertial effects. Int. Comm. Heat Mass Transfer 2002; 29: 879–885.
32. Jansen, K.M.B., De Vreugd, J., Ernst, L.J. Analytical estimate for curing-induced stress and warpage in coating layers. J. Appl. Polym. Sci. 2012; 126: 1623–1630.
33. Polyakov W.A., Pierov J.J. Экспериментальные методы оценки кромочного эффекта, Mech. Compos. Mater. 1989; 2: 318–331.
34. Paramonov, Y.M., Kleinhof, M.A., Paramonova, A.Y. Markov Model of Connection Between the istribution of Static Strength and Fatigue Life of a Fibrous Composite, Mech. Compos. Mater. 2006; 42(5): 615–630.
35. Pascual, F.G., Meeker W.Q. Technometrics 1999; 41: 277–302.
36. Chatys, R., Paramonova, A.Y., Kleinhof, M.A. Analysis of Residual Strength afterFatigue in Fibrous Composite using Markov Chains Mode. Monography: Selected Problems of Modeling and Control in Mechanics. Edited by St. Adamczak and L. Radziszewski, Kielce 2011; 166–178.
37. Paramonov, J., Chatys, R, Andersons, J., Kleinhofs, M. Poisson process of defect initiation in fatigue of a composite material, 2011, International Conferences „RelStat'2011",Riga, Latvia 2011; 1–12.
38. Chatys, R. Statistical verification of strength parameters of fibrous composite materials. Quarterty "Composites theory and practice" 2012; 12(3): 171–176.
39. Fleming, W.H., Soner, H.M. Controlled Markov processes and viscosity solutions. New York. Springer Verlag 1993
40. Chatys, R. Investigation of the Effect of Distribution of the Static Strength on the Fatigue Failure of a Layered Composite by Using the Markov Chains Theory. Mechanics of Composite Materials 2012; 48(6): 911–922.
41. Dekker, R., Nicolai, R.P., Kallenberg, L.C.M. Maintenance and Markov decision models. In Wiley StatsRef: Statistics Reference Online (eds Balakrishnan N, Colton T, Everitt B, Piegorsch W, Ruggeri F, Teugels J.L.). John Wiley & Sons 2014. DOI: 10.1002/9781118445112.stat03960
42. Found, M.S., Quaresimin, M. Two–stage fatigue loading of woven carbon fiber reinforced laminates, Fatigue Fract. Eng. Mater. Struct. 2003; 26: 17–26.
43. Paramonov, J., Chatys, R., Anderson, J. Kleinhofs M. Markov Model of Fatigue of a Composite Material with Poisson Process of Defect Initiation, Mechanics of Composite Materials 2012; 48(2): 211–228.
44. Wu, X., Zou, X., Guo, X. First passage Markov decision processes with constraints and varying discount factors. Frontiers of Mathematics in China 2015; 10(4): 1005–1023. https://doi.org/10.1007/s11464–015–0479–6
45. Chatys, R. Application of the Markov Chain Theory in Estimating the Strength of Fiber-Layered Composite Structures With Regard to Manufacturing Aspects. Advances in Science and Technology Research Journal 2020; 4(4): 64–71.
46. Macek, W. Fractal analysis of the bending-torsion fatigue fracture of aluminium alloy. Engineering Failur Analysis 2019; 99: 97–107. DOI: 10.1016/j.engfailanal.2019.02.007
47. Macek, W., Martins, R.F., Branco, R., Marciniak, Z., Szala, M., Wroński, S. Fatigue fracture morphology of AISI H13 steel obtained by additive manufacturing. International Journal of Fracture 2022; 235: 79–98. DOI: 10.1007/s10704–022–00615–5
48. Vautard, F., Ozcan, S., Poland, L. Influence of thermal history on the mechanical properties of carbon fiber-acrylate composites cured by electron beam and thermal processes. Compos. Part A Appl. Sci. Manuf. 2013; 45: 162–172.
49. Szumniak, J., Smoczyński, Z., Szcześniak, K. Aging of polymer composites of armaments and military equipment. WSOWL 2011; 159(1): 271–285.
50. Chatys, R., Orman, Ł.J. Technology and properties of layered composites as coatings for heat transfer enhancement. Mechanics of Composite Materials 2017; 53(3): 351–360.